Desalination and Water Treatment
www.deswater.com

doi: 10.5004/dwt.2021.27313

228 (2021) 198–207
July

Investigation of intrinsic bisphenol separation capacity of zeolitic imidazolate framework-8 based membranes

Sujithra Sundarajan[a], Yohannan Subin Sabilon[a], G. Arthanareeswaran[a,*], Wirach Taweepreda[b]

[a]*Membrane Research Laboratory, Department of Chemical Engineering, National Institute of Technology Tiruchirappalli, India, email: arthanaree10@yahoo.com (G. Arthanareeswaran)*
[b]*Department of Material Science and Technology, Faculty of Science, Prince of Songkla University (PSU), Hat Yai, Songkla 90110, Thailand*

Received 15 October 2020; Accepted 7 March 2021

ABSTRACT

The present study deals with the synthesis of polyetherimide (PEI)-based membrane with zeolitic imidazolate framework (ZIF) nanoparticles as fillers by wet phase technique. The synthesized membranes were characterized based on their physical and chemical properties and were used to study the effective removal of Bisphenol A (BPA) from water. After the BPA removal with different membrane compositions, it was found that 1% PEI/ZIF-8 mixed matrix membrane gave maximum BPA rejection of 94.1% in comparison with other membranes. The flux recovery ratio of 0.92 was also found to be the highest for 1% PEI/ZIF-8 membrane which shows that this membrane has undergone the least fouling when compared to other membrane compositions. Overall, a 1% concentration of PEI/ZIF-8 membrane showed better characteristics and a maximum percentage of BPA removal was obtained.

Keywords: Bisphenol A; Mixed matrix membranes; Polyetherimide, Zeolitic imidazolate frameworks; Rejection

1. Introduction

Endocrine-disrupting chemicals (EDCs) are organic compounds that can cause abnormalities in the functioning of the endocrine system are of great public and environmental concern [1]. It was reported that EDCs disturb the endocrine system by mimicking, blocking or disrupting the functions of hormones mostly. As a result of this, they affect the health of humans and animal species badly [2]. Bisphenol A (BPA) is identified as one of the most important endocrine-disrupting chemicals with one or more phenolic groups which have gained more importance in chemical industries. BPA is primarily used as an intermediate in the production of polycarbonate plastics and epoxy resins, phenol resins, flame retardants, polyacrylates, polyesters and lacquer coating on food cans [3,4]. BPA was first reported by Dianin in 1891 and then synthesized by Zincke in 1905 from phenol and acetone [5]. During the past decades, a variety of techniques have been used for the removal of BPA such as adsorption [6], ozonation [7], Fenton degradation [8], photocatalytic decomposition [9], electrochemical oxidation [10], UV/H_2O_2 oxidation [11] and biodegradation. Among these techniques, membrane separation is generally considered to be the most efficient method for the rapid removal of BPA from wastewater or effluent. There are different mechanisms like sieving, adsorption and electrostatic interaction in the membrane separation process for the elimination of micropollutants. The mechanisms of BPA elimination in nanofiltration and reverse osmosis membrane are established on sieving and electrostatic interaction [12] while the elimination mechanism in microporous microfiltration and ultrafiltration is

* Corresponding author.

directed by adsorption [13] Research revealed that around 90% BPA elimination could be achieved using membrane technology. The characteristics of BPA, feed water, membrane properties and operating conditions are the factors to be known which influence the removal of BPA from water during the membrane process [14]. Membrane technology has experienced substantial growth and advances during the past decades with attractive features like high energy efficiency, simplicity in design, construction of membrane modules and environmental compatibility. In this study, selected membranes were tested and compared for their performances in BPA rejection from water.

Polyetherimide (PEI) is a commercial membrane material that has extensive application in various industrial processes owing to its excellent chemical resistance, good processability and high tensile strength over a wide range of temperatures. Zeolitic imidazolate framework (ZIF) nanocrystals when combined with PEI polymer provides more selectivity and enhances the chemical stability of the membrane, since in order to be used against BPA. This additive can also easily alter the pore structure in such a way that it is compatible with the chosen polymer [15]. The modifications in PEI membrane is achieved through methods like coating, physical blending, interfacial polymerization by modifying the surface, grafting, etc. when compared to other methods of modifications, blending is more appropriate to synthesize easily and provides uniform structure while the other modification methods are very expensive and require harsh conditions like acidic or alkaline conditions [16,17].

In this study, six different concentrations of ZIF-8 nanocrystals varying from 0% to 2.5% were used as inorganic fillers in the PEI polymer matrix. N-methyl-2-pyrrolidone (NMP) was used as a solvent to prepare the casting solution for the fabrication of these membranes. The synthesized membranes are characterized to study their physical and chemical properties. Fourier-transform infrared spectroscopy (FTIR) analysis confirmed the presence of ZIF-8 nanocrystals in the composite membrane. The cross-sectional and top surface morphology of the membranes were studied by scanning electron microscopy (SEM) images. Material strength tests were done to determine the physical strength of the membranes. Contact angle tests were done to determine the nature of the membrane. Porosity determination tests were done to determine the number of pores present per unit area of the membrane. The aim of this work was to determine the best possible combination of the mixed matrix membrane that can be used for BPA separation from water, so different protein rejection studies, determination of flux recovery ratio and the surface energy calculations were done for this purpose.

2. Materials and methods

2.1. Materials

Zinc hydrate crystals and NMP required in the preparation of ZIF-8 nanocrystals were purchased from Merck Life Science Private Limited, Mumbai, India. Methanol used for washing during centrifugation was bought from Titan Biotech Limited, Rajasthan, India. The chemicals 2-methylimidazole and n-butylamine required for the preparation of ZIF-8 nanocrystals were bought from Otto Group, Hamburg, Germany. PEI polymer was purchased from Solvay Specialty Polymers, Malaysia. Acetone was purchased from Merck Specialities Private Limited, Mumbai, India. All reagents were used without any further purification.

2.2. Experimental section

2.2.1. Preparation of ZIF-8 nanocrystals

The 734.4 mg of zinc hydrate, that is, $Zn(NO_3)_2 \cdot 6H_2O$ crystals was taken in a conical flask containing 50 mL of methanol. The conical flask was then kept on a magnetic stirrer for complete dissolution. Now two beakers were taken, in one beaker 50 mL of methanol was taken to which 0.975 mL of n-butylamine was added while in the second beaker 810.6 mg of 2-methylimidazole was taken and the contents of the former beaker were poured into the latter one. Then the mixture so formed in the latter beaker was poured into the conical flask while under constant stirring. The stirring was continued to obtain a uniform solution. After a while, the stirring was stopped and the contents of the conical flask were allowed to settle. The mouth of the conical flask was covered using cotton or aluminum foil to prevent contamination from the surrounding. After 24 h of standing still, gel-like solid is settled at the bottom of the conical flask. The gel-like solid was recovered from centrifugation and then washed with methanol. The centrifugation is repeated 3 times. After centrifugation, the particles were dried at room temperature and were ground into a fine powder and the ZIF-8 nanocrystals were formed. The confirmation of these ZIF-8 nanoparticles was done using UV spectroscopy and X-ray diffraction (XRD) analysis while the morphology of these particles was studied by transmission electron microscopy (TEM) and SEM analysis.

2.2.2. Preparation of PEI/ZIF-8 membranes

The ZIF-8 nanocrystals were chosen as a modifier to evaluate the performance of the PEI membrane. The total polymer casting solution constitutes 20 wt.% of PEI along with the varying composition of ZIF-8 crystals, which are dissolved in NMP. The dope solution is mixed by constant mechanical stirring at 60°C for a time period of 3–4 h. This homogenized solution is cast on a glass plate using a thin film applicator which is set to a thickness of 250 μm. An idle time of 30 s for the thin film on the glass plate, allows partial solvent evaporation under room temperature. Subsequently, it is immersed in a 3% sodium dodecyl sulfate solution for a period of 12 h. The additive compositions of polymer and inorganic filler has taken for respective concentrations are shown in Table 1.

2.2.3. Preparation of synthetic BPA solution

The BPA was synthetically prepared by adding 50 mg of BPA in 1 L of water [18]. Once 50 mg/L of BPA solution was prepared the solution was concentration determination was done at different pH. This is necessary as at very high and very low pH the BPA undergoes hydrolysis therefore it is important to determine at what pH the BPA

Table 1
Composition of PEI/ZIF-8 membranes

Concentration of PEI/ZIF-8 membranes (wt.%)	Amount of PEI (g)	Amount of ZIF-8 nanocrystals (g)
0	4.375	0
0.5	4.353	0.022
1	4.331	0.043
1.5	4.309	0.065
2	4.287	0.087
2.5	4.265	0.109

separation must be carried out. The pH of the solution was decreased and increased by adding HCl and NaOH respectively. The absorbance of the 50 mg/L BPA solution was then determined at different pH using UV Visible Spectroscopy and a graph was plotted to show the variation of absorbance with different pH of the solution and the pH at which the BPA separation should take place was determined.

2.2.4. Separation of BPA from water using PEI/ZIF-8 membranes

A dead-end filtration set up as shown in Fig. 1 was used for the separation process. The concentration of BPA in the feed is 50 mg/L. The pressure maintained for the separation process was 10 bar [13]. The water flux and the BPA separation experiments were done for membranes with different inorganic filler concentrations. The different parameters of separation were studied and the best membrane composition for the separation of BPA from the water was determined.

After the separation was done the permeate flux and the BPA rejection of the individual membranes were calculated by using the formula given below [13]:

$$\text{Rejection of BPA} = \left(1 - \frac{C}{C_f}\right) \times 100 \tag{1}$$

$$\text{Permeate flux} = \frac{V}{A \times t} \tag{2}$$

2.3. Membrane characterization

Hydrophilicity is measured using contact angle measurement. The contact angle is determined by the sessile drop method using a goniometer (model 250-F1 Rame Hart Instruments, Succasunna, NJ). About 5 μL drop of water is injected on a dry membrane surface at five different locations through a microsyringe. The average contact angle value was measured from the individual droplets in the five regions which determine the hydrophilicity of the membrane. Any presence of chemical functional groups over the membrane surface was identified using attenuated total reflectance-Fourier transform infrared (ATR-FTIR) spectroscopy (Thermo Scientific Nicolet iS5 FTIR spectrometer). The spectra for all the dried membrane samples are observed in the wavelength range of 4,000–400 cm^{-1}.

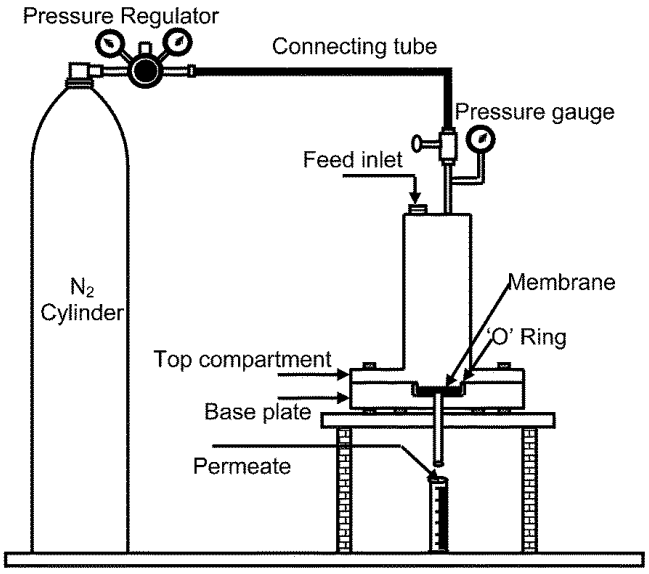

Fig. 1. Dead-end filtration setup.

The cross-sectional morphology of the membranes is observed using SEM (JEOL JSM-5600 SEM) at 15 kV. Membrane samples are coated with platinum powder on the surface. Thermal stability is observed using a thermal analyzer (model SDT 2000, New Castle, DE). Thermal analysis-based membrane characterization is executed under a temperature range of 25°C–600°C gradually ramped at a rate of 10°C/min in a nitrogen-controlled atmosphere. To measure the porosity of the membrane, samples were cut into specific sizes and then mopped with filter paper. After noting their wet weight, the samples are dried in an oven at 60°C for 24 h. The porosity and mean pore radius of the membranes were calculated by Eqs. (1) and (2) respectively. To test the maximum tensile stress, the membrane under test is cut into two dumbbell-shaped pieces. For performing this analysis, ASTM D412 standard method was followed using a uniaxial mechanical testing machine (Instron, Canton, MA). XRD analysis and TEM analysis were performed to confirm the presence of ZIF-8 nanocrystals in the membrane and the size of these organic fillers in the membrane respectively. The surface energy of the membranes were calculated based on the contact angles of each membrane. It was calculated by using the formula given below [15]:

$$-\Delta G_s = \left(1 + \text{Cos}\theta\right)\Upsilon_L^T \tag{3}$$

The FRR determination is done to determine the fouling withstanding capacity of the membranes. The higher the FRR of a membrane the lower the fouling. Therefore, the membrane with least fouling was determined using this procedure.

The FRR of the membrane was calculated by using the formula given below [15]:

$$\text{Flux recovery ratio} = \frac{J_f}{J_i} \tag{4}$$

where initial water flux = J_i; final water flux = J_f.

2.3.1. Protein rejection studies

The protein rejection studies were done by using 3 different proteins of different sizes namely lysozymes (14 kDa), egg albumin (44 kDa) and BSA (66 kDa). The protein rejection studies were done to determine the molecular weight cut-off (MWCO) the membranes. The separation of these proteins was carried out using membranes of different compositions and if 80% of protein is rejected by the membranes, we can say that the MWCO of the membranes is same as that of the size of the protein that is being separated, thus the MWCO of the membranes can be determined.

3. Results and discussion

3.1. FTIR analysis of PEI/ZIF-8 membranes

The FTIR results shown in Fig. 2 show the presence of aluminosilicates in the PEI/ZIF-8 in the prepared membranes. The aluminosilicate bonds are present due to the presence of ZIF-8 nanoparticles. The presence of aluminosilicate bonds in the FTIR graph confirms the presence of ZIF-8 nanoparticles present in the membrane while the presence of ester, ketones, amines and organosulphur confirms the presence of PEI polymer in the membrane. As the ZIF-8 nanoparticles have good selectivity for BPA separation, so it can be proposed that the developed PEI/ZIF-8 membranes can be used for BPA separation from water.

3.2. Cross-sectional morphology of PEI/ZIF-8 membranes

Fig. 3 shows the SEM images of the PEI/ZIF-8 mixed matrix, which indicates good contact of bare ZIF-8 to the PAI matrix at each loading. Excellent contact was obtained without any surface treatment of the sieve. The SEM images of PEI/ZIF-8 mixed matrix are different than well-dispersed 10 nm ZIF-8 particles. There also exist many non-ideal arrays of ZIF-8 with sizes varying from 50 nm to several microns, which is greater than an order of magnitude larger than single ZIF-8 particles. Also, the volume fraction of large ZIF-8 arrays in the matrix increases with increasing ZIF-8 loading. No defects were seen for these arrays among all the PEI/ZIF-8 dense film samples.

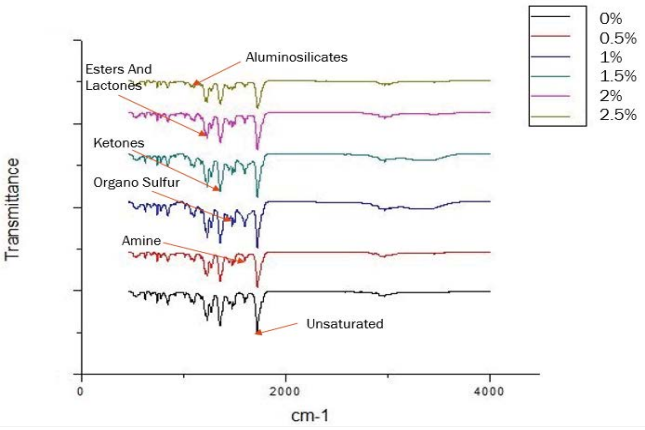

Fig. 2. FTIR analysis of PEI/ZIF-8 membranes.

By achieving the desired uniform distribution of individual ZIF-8 particles with the PEI matrix outstanding BPA separation results can be achieved. The cross-sectional view of the PEI/ZIF-8 membranes shows good adhesion between the inorganic filler ZIF-8 and the polymeric membrane PEI [15]. The figures show the SEM images of 0%, 0.5%, 1%, 1.5%, 2% and 2.5% PEI/ZIF-8 membranes prepared respectively. The cross-sectional view of the ZIF 8/PEI membranes shows the uniform porous structure of the membranes.

3.3. Top surface morphology of PEI/ZIF-8 membranes

Scanning electron micrographs of the top surface of PEI/ZIF-8 membranes is shown in Fig. 4. The polymeric film has been observed at very high resolution under SEM. High magnification of the wall in the cross-section of the PEI/ZIF-8 reveals a gradual transition from the porous inner core to the denser outer micropore structure. In contrast, high magnification of the top surface of PEI/ZIF-8 shows a uniform dense micropore structure in Fig. 4b. These micrographs demonstrate smaller ZIF-8 particles (mostly <1 μm) with uniform distribution of these particles, as well as excellent polymer–sieve contact. The top surface view of the PEI/ZIF-8 membranes shows good adhesion between the inorganic filler ZIF-8 and the polymeric membrane PEI [15].

3.4. Contact angle test

The contact angle for all the membranes with different filler concentrations was determined by using a goniometer. The contact angle of each of these membranes was calculated by taking the mean value of the left and right angle of the membranes and the results are given in Table 2. As the contact angle of the membrane goes on increasing the membrane becomes more and more hydrophobic in nature. So, from the data obtained it is observed that as the filler concentration increases the membrane becomes more hydrophilic in nature [16,17]. Since the contact angle measurements are less than 90°, we can confirm that the membranes are hydrophilic in nature [18,19].

3.5. Stress-strain analysis

The material strength of the membranes prepared was studied by performing stress-strain tests. The Universal Testing Machine was used to perform the tests. The data was recorded for respective samples and tabulated in Table 3. It can be observed that as the concentration of the ZIF-8 nanoparticles in the membrane increases the ultimate strain that the membrane can withstand decreases. This is due to the agglomeration caused by adding excessive concentrations of ZIF-8 particles. Therefore, the membranes tend to become more and more brittle in nature as the ZIF-8 concentration increases. In comparison of the stress-strain results of the different membrane compositions it can be seen that 0.5% PEI/ZIF-8 can withstand an ultimate strain of 15.2% while 1% PEI/ZIF-8 can withstand an ultimate strain of 10.9%. So, it can be concluded that with respect to material strength 0.5% PEI/ZIF-8 membranes is better than 1% PEI/ZIF-8 membranes for BPA separation from water.

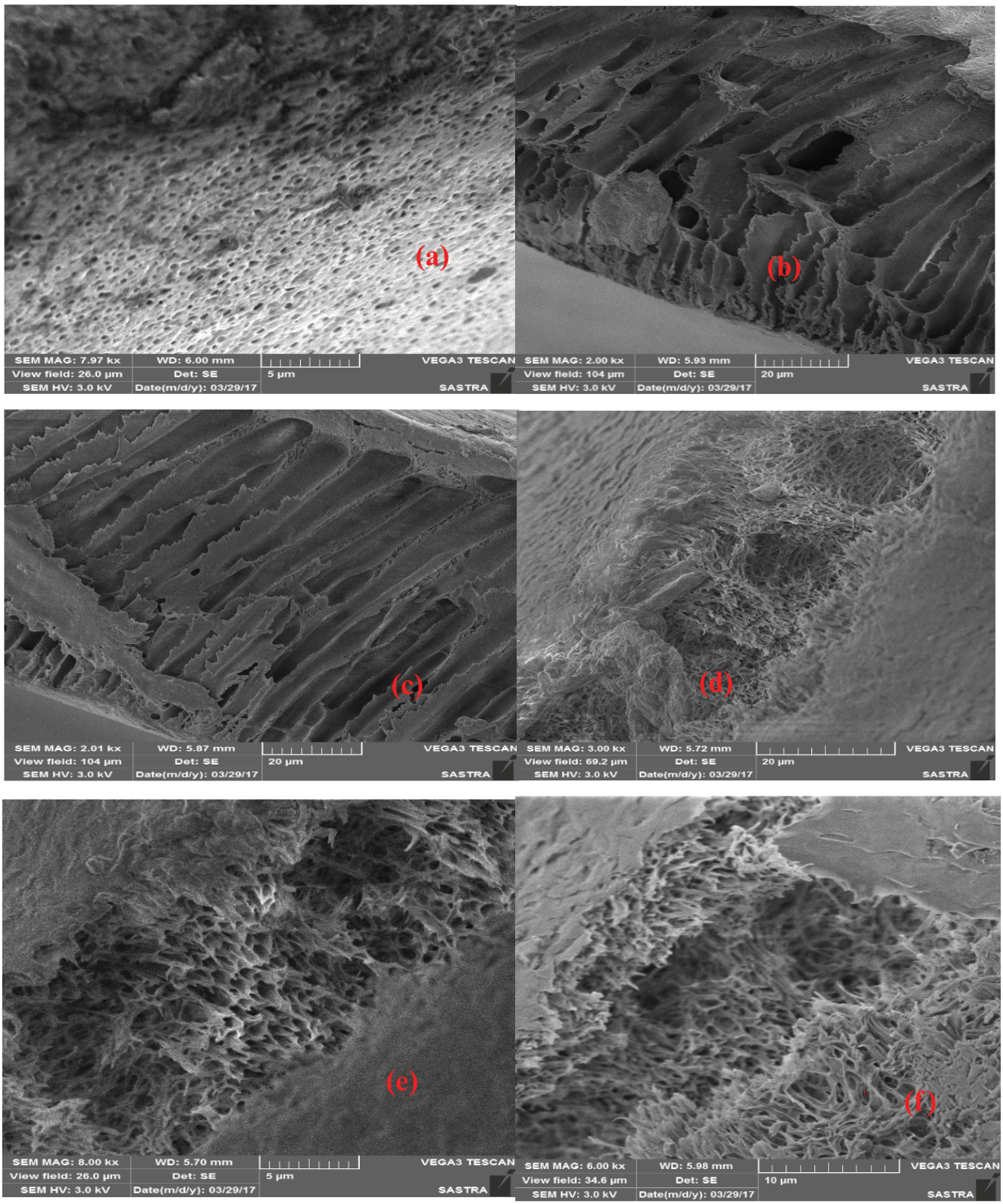

Fig. 3. Cross-sectional morphology of PEI/ZIF-8 membranes – (a) 0%, (b) 0.5%, (c) 1%, (d) 1.5%, (e) 2%, and (f) 2.5%.

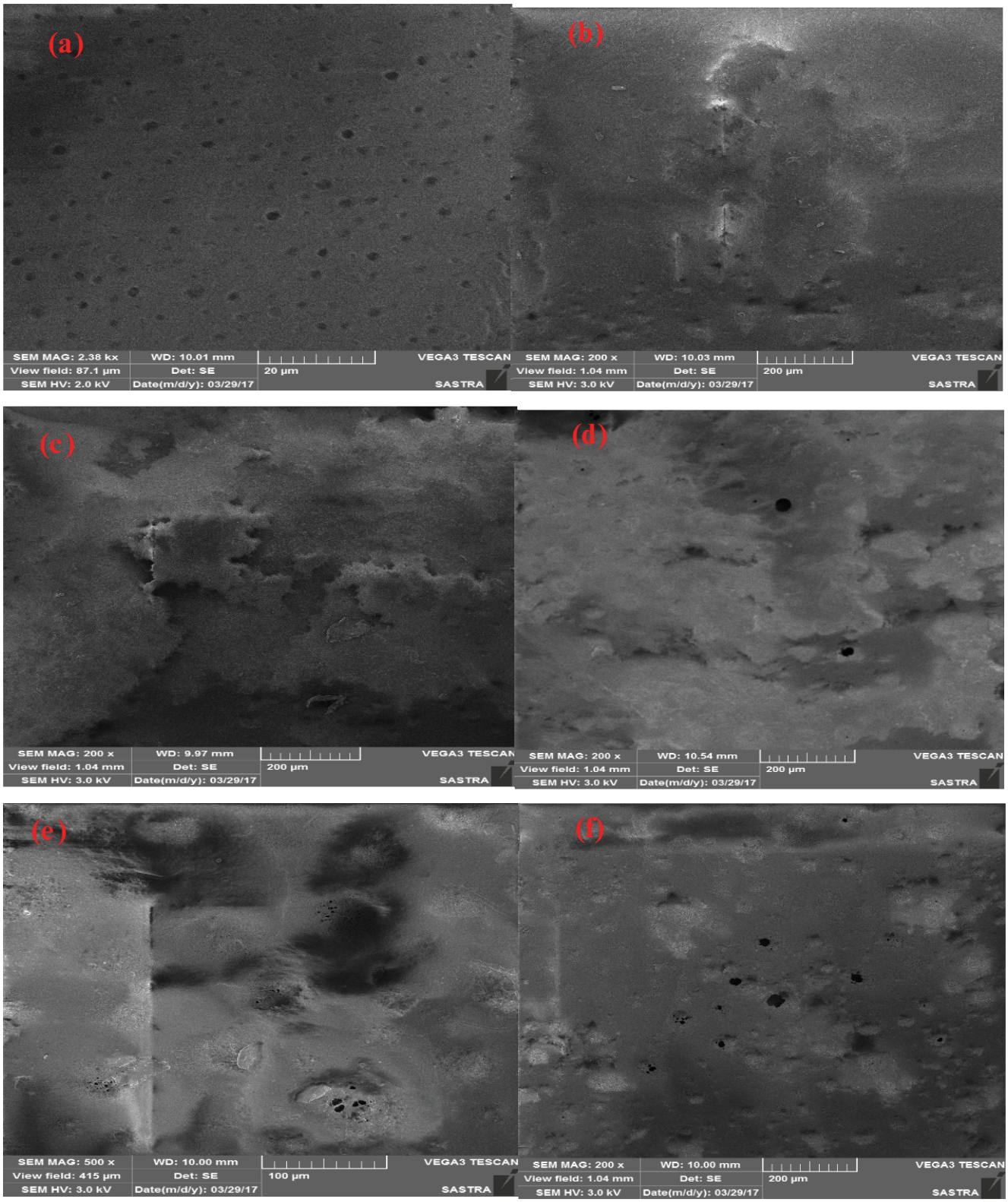

Fig. 4. Top-surface morphology of PEI/ZIF-8 membranes – (a) 0%, (b) 0.5%, (c) 1%, (d) 1.5%, (e) 2%, and (f) 2.5%.

3.6. Porosity

The porosity and mean pore radius values are shown in Table 4. The average pore radius of PEI/ZIF-8 membrane has been increased from 5.23 to 9.97 nm and the porosity (%) value also increases from 86% to 94% due to the addition of ZIF-8 nanoparticles into PEI casting solution. The change in porosity is due to the good MOF structure of the nanoparticles used. The results confirm the hydrophilic nature of the membrane. The increasing concentration of the inorganic fillers increases the membrane water absorption capacity which leads to an increase in fouling resistant property of the membrane [20].

3.7. UV-visible spectroscopy analysis of BPA sample

Fig. 6 shows the variation of the absorbance value of the BPA sample with the wavelength. The concentration of BPA in the feed was determined by using UV-Visible spectroscopy. The absorbance value at 276 nm peak was determined and the concentration of BPA in the feed as well as the permeate was determined [18].

3.8. BPA rejection studies

The BPA separation from the water was carried out for different membrane compositions. Initially, the pH and UV spectroscopy analysis were carried out for the BPA sample solution and the results were shown in Figs. 5 and 6, respectively. The concentration of BPA in the permeate, permeate flux and the BPA rejection was evaluated at regular intervals of time. The different graphs showing the variation of concentration of BPA in the permeate, permeate flux and BPA rejection with respect to time and filler concentration are given in Figs. 7–10.

It can be seen from Fig. 7 that as the inorganic filler concentration increases the rejection of BPA also increases, this is due to the increase in the selectivity of the membranes due to the presence of ZIF-8 nanocrystals. But after 1% PEI/ZIF-8 membrane, the further increase in the filler concentration decreases the rejection of BPA [21]. This is due to the increased porosity for higher concentration membranes as BPA doesn't get adsorbed on the membrane and passes through the membrane pores to the permeate. It can also be seen that as time increases the rejection of BPA for all the membranes decreases as all the water has come out as the permeate [19].

It is observed from Fig. 8 that as time increases the concentration of BPA in the permeate also increases as all the water has come out as permeate therefore on the continuous application of pressure the BPA passes through the membrane pores and comes out as permeate. It can also be seen that as the concentration of filler in the

Table 2
Contact angle results

Membrane composition	Left	Right	Mean
0%	70.8	71.8	71.3
0.5%	70.4	69.5	69.9
1%	76.9	78.7	77.8
1.5%	75.5	74.3	74.9
2%	78.1	78.1	78.1
2.5%	71.4	70.6	71.0

Table 3
Stress-strain results

Membrane composition	Break distance (mm)	Ultimate force (N)	% Total elongation	Ultimate stress (MPa)	Yield stress (MPa)	Ultimate strain (%)
0%	0.734	2.93	7.34	0.587	–	2.88
0.5%	1.57	8.03	15.7	1.61	–	15.2
1%	1.10	7.37	11.0	1.47	–	10.9
1.5%	0.330	5.22	3.30	1.04	1.04	3.26
2%	0.955	7.37	9.55	1.47	1.47	9.26
2.5%	0.717	8.17	7.17	1.63	–	6.85

Table 4
Porosity of different membrane compositions

Inorganic filler used (%)	Wet weight of the membrane (g)	Dry weight of the membrane (g)	Amount of water absorbed (g)	Porosity
0	0.0394	0.0067	0.0327	0.861
0.5	0.0464	0.0067	0.0397	0.882
1	0.0432	0.0062	0.0370	0.883
1.5	0.0379	0.0065	0.0314	0.859
2	0.0446	0.0061	0.0385	0.948
2.5	0.0420	0.0065	0.0355	0.873

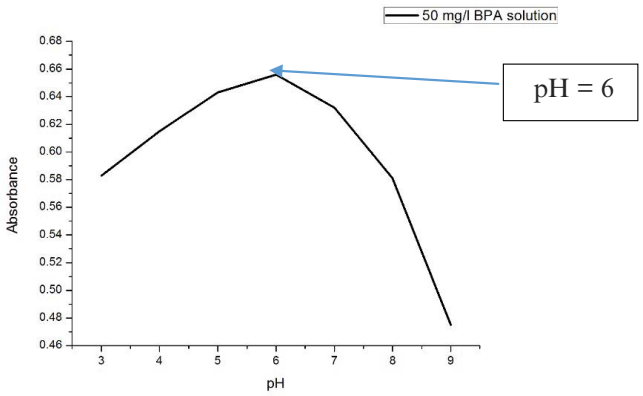

Fig. 5. Effect of pH on the determination of 50 mg/L BPA sample.

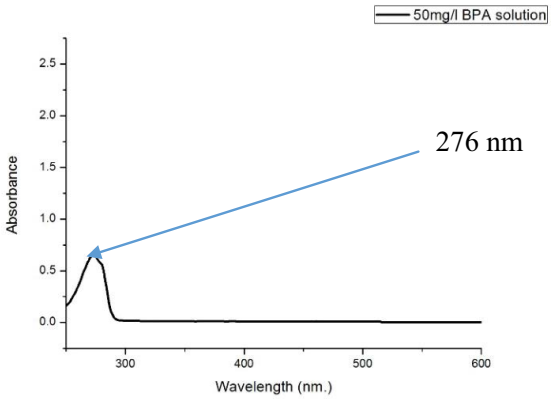

Fig. 6. UV-Visible spectroscopy analysis of BPA sample.

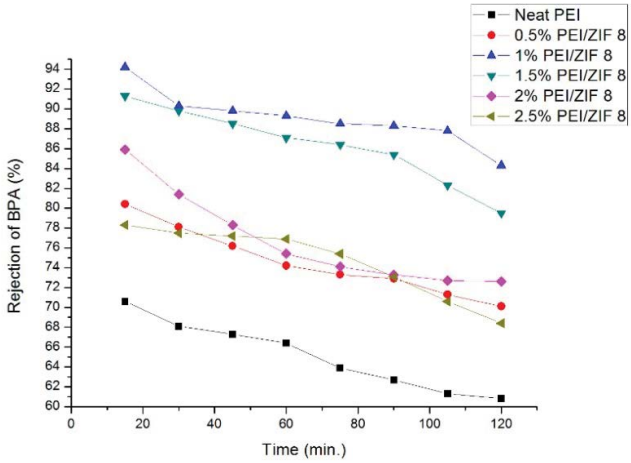

Fig. 7. BPA rejection vs. time.

membrane increases the concentration of BPA in the permeate decreases as the selectivity of the membranes increases the BPA gets adsorbed on the membrane surface. But after 1% PEI/ZIF-8 membrane, the further increase in the filler concentration increases the concentration of BPA in the permeate this is due to the increased porosity for higher concentration membranes as BPA doesn't get adsorbed

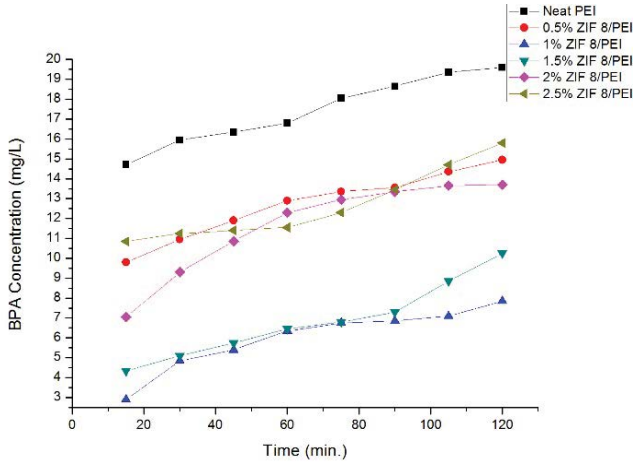

Fig. 8. BPA concentration vs. time.

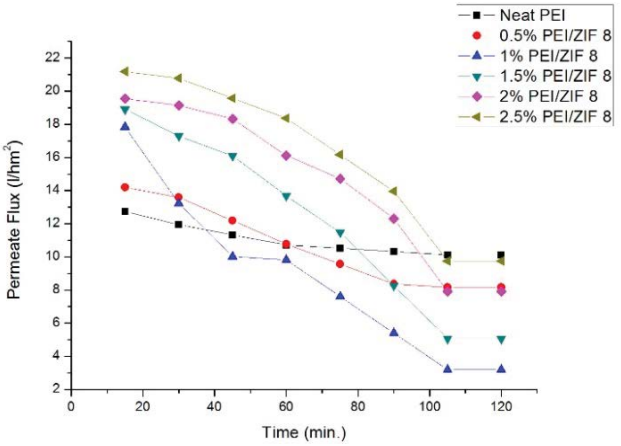

Fig. 9. Permeate flux vs. time.

on the membrane and passes through the membrane pores to the permeate [13].

It can be seen from Fig. 9 that as the time increases the permeate flux of all the membranes decreases as the fouling of each membrane takes place as BPA gets adsorbed on the membrane surface. It can also be seen that the initial permeate flux of membranes increases as the filler concentration increases due to the increase in the porosity of the membranes.

Fig. 10 shows that as the permeate flux decreases for all the membranes the rejection of BPA also decreases as all the water has come out as permeate therefore on the continuous application of pressure the BPA passes through the membrane pores and comes out as permeate. It can also be seen from the figure that as the inorganic filler concentration increases the rejection of BPA also increases, this is due to the increase in the selectivity of the membranes due to the presence of ZIF-8 nanocrystals. But after 1% PEI/ZIF-8 membrane, the further increase in the filler concentration decreases the rejection of BPA this is due to the increased porosity for higher concentration membranes as BPA doesnot get adsorbed on the membrane and passes through the membrane pores to the permeate. At 120 min,

the rejection of neat PEI is 61%, the rejection performances of fabricated membranes with 1% ZIF-8 were increased significantly to 84%. This is ascribed to electrostatic repulsion between ZIF-8 loaded PEI membrane surface and dissociated BPA (–O–) group. The HA molecules occupied an active site on the membrane surface and the presence of ZIF-8 in the membrane exhibits a lesser active site for BPA molecules noticed in the BPA rejection.

According to Fig. 10, the permeate flux and BPA rejection decreased with increasing the BPA concentration. At high BPA concentration, excess BPA molecule shields the ZIF-8 charge that weakens the electrostatic repulsion and reduces rejection. When the concentration of HA increased, HA forms as a layer that forms hydrophobic interactions among hydrophobic compounds and hinders the diffusion of BPA molecule [22].

3.9. Protein rejection studies

The protein rejection studies were done to determine the MWCO of the membranes. The protein separation experiments for each membrane composition were carried out and their respective rejection was determined and the values are shown in Table 5. Since all the membranes reject more than 80% of the proteins, therefore, it was found that the MWCO of all the membranes is 14 kDa.

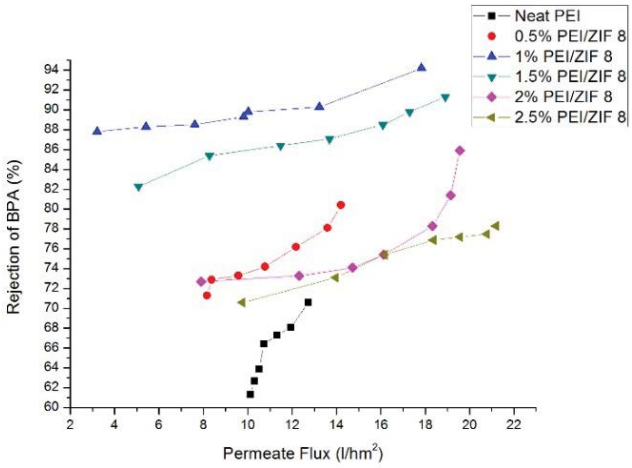

Fig. 10. BPA rejection vs. permeate flux.

3.10. Surface free energy calculation

The contact angle for all the membranes with different filler concentrations was determined by using a goniometer. The surface free energy of each of these membranes was calculated by using their respective contact angle values and the results are given in Table 6. As the contact angle of the membrane goes on increasing the membrane becomes more and more hydrophobic in nature. So, it can be seen that as the filler concentration increases the membrane becomes more hydrophilic in nature [23]. The hydrophilic property of the membrane increases the surface free energy of the membrane thereby it reduces the interaction between the feed and the membrane. So as the filler concentration in the membrane increases the adsorption of BPA on the membrane decreases.

3.11. FRR determination

The experiments to determine the initial and final water flux of all the membranes were done and the results are tabulated in Table 7. The FRR of each membrane was calculated and it was found that the FRR increased as the ZIF-8 nanoparticle concentration in the membrane was increased, this was due to the increase in the porosity of the membrane as the filler concentration increases. But after 1% PEI/ZIF-8 membrane, the further increase in the filler concentration decreases the FRR this is due to the increased fouling for higher concentration membranes as BPA gets adsorbed on the membrane and blocks the pores of the membrane. Since the flux recovery ratio of 1% PEI/ZIF-8 is high, the

Table 6
Surface free energy of different membrane composition

Membrane composition	Mean contact angle	Surface free energy ($-\Delta G_s$) in mJ/m²
0%	78.1°	87.81
0.5%	77.8°	88.18
1%	74.9°	91.76
1.5%	71.3°	96.14
2%	71.0°	96.50
2.5%	69.9°	97.82

Table 5
Protein rejection studies

Membrane composition	Rejection of proteins (%)		
	Lysozymes (14 kDa)	Egg albumin (44 kDa)	BSA (66 kDa)
0%	81.23	89.37	94.22
0.5%	87.84	92.36	94.82
1%	89.83	92.84	93.82
1.5%	82.34	89.38	93.76
2%	87.93	91.49	94.28
2.5%	83.49	90.34	92.38

Table 7
FRR determination of different membrane composition

Membrane composition	Initial water flux (J_i)	Final water flux (J_f)	Flux recovery ratio = J_f/J_i
0%	15.793	12.739	0.773
0.5%	17.022	14.202	0.835
1%	19.381	17.831	0.920
1.5%	21.409	18.904	0.883
2%	23.255	19.552	0.840
2.5%	25.811	21.181	0.821

fouling is the lowest for this membrane as the FRR is inversely proportional to membrane fouling.

4. Conclusions

In this study, the synthesis of ZIF-8 nanocrystals and the various tests required to prove the confirmation of these particles were done. The ZIF-8 nanocrystals have a rhombic dodecahedral crystal structure and the size of the crystals was less than 100 nm. The mixed matrix membrane fabrication using ZIF-8 nanocrystals as fillers was also done successfully and the various characterization tests show that the membranes can be used for BPA separation from water. As the concentration of inorganic fillers increased, the PEI/ZIF-8 membranes provide high thermal and chemical stability along with a good membrane structure, permeability and selectivity. The various tests for permeation, permeability and selectivity were done for different concentrations of PEI/ZIF-8 membranes. The performance of all the membranes was compared and it was found that for 1% PEI/ZIF-8 membrane BPA rejection was 94.1% which is maximum in comparison with other membranes while the flux recovery ratio was found to be 0.920 which means its fouling is minimum on comparison with other membranes. Therefore, we can conclude that a 1% PEI/ZIF-8 membrane is best suited for BPA removal from water in comparison with other membranes.

References

[1] Y.Q. Huang, C.K.C. Wong, J.S. Zheng, H. Bouwman, R. Barra, B. Wahlström, L. Neretin, M.H. Wong, Bisphenol A (BPA) in China: a review of sources, environmental levels, and potential human health impacts, Environ. Int., 42 (2012) 91–99.

[2] N. Bolong, A.F. Ismail, M.R. Salim, D. Rana, T. Matsuura, A. Tabe-Mohammadi, Negatively charged polyethersulfone hollow fiber nanofiltration membrane for the removal of Bisphenol A from wastewater, Sep. Purif. Technol., 73 (2010) 92–99.

[3] C.A. Staples, P.B. Dorn, G.M. Klecka, S.T. O'Block, L.R. Harris, A review of the environmental fate, effects, and exposures of Bisphenol A, Chemosphere, 36 (1998) 2149–2173.

[4] T. Yamamoto, A. Yasuhara, H. Shiraishi, O. Nakasugi, Bisphenol A in hazardous waste landfill leachates, Chemosphere, 42 (2001) 415–418.

[5] J.S. Moore, X. Prat-Resina, Tim Wendorff, E. V., John W., Hahn, A., Bisphenol A, 2020. Available at: https://chem.libretexts.org/@go/page/5083

[6] I. Bautista-Toledo, M.A. Ferro-García, J. Rivera-Utrilla, C. Moreno-Castilla, F.J. Vegas Fernández, Bisphenol A removal from water by activated carbon. Effects of carbon characteristics and solution chemistry, Environ. Sci. Technol., 39 (2005) 6246–6250.

[7] M. Umar, F. Roddick, L.H. Fan, H.A. Aziz, Application of ozone for the removal of Bisphenol A from water and wastewater – a review, Chemosphere, 90 (2013) 2197–2207.

[8] X.J. Yang, P.-F. Tian, C.X. Zhang, Y.-Q. Deng, J. Xu, J.L. Gong, Y.-F. Han, Au/carbon as Fenton-like catalysts for the oxidative degradation of Bisphenol A, Appl. Catal., B, 5 (2013) 145–152.

[9] C.Y. Wang, H. Zhang, F. Li, L.Y. Zhu, Degradation and mineralization of Bisphenol A by mesoporous Bi_2WO_6 under simulated solar light irradiation, Environ. Sci. Technol., 44 (2010) 6843–6848.

[10] Y.-H. Cui, X.-Y. Li, G.H. Chen, Electrochemical degradation of Bisphenol A on different anodes, Water Res., 43 (2009) 1968–1976.

[11] R.A. Torres, C. Pétrier, E. Combet, F. Moulet, C. Pulgarin, Bisphenol A mineralization by integrated ultrasound-UV-iron (II) treatment, Environ. Sci. Technol., 41 (2007) 297–302.

[12] Y. Zhang, C. Causserand, P. Aimar, J.P. Cravedi, Removal of Bisphenol A by a nanofiltration membrane in view of drinking water production, Water Res., 40 (2006) 3793–3799.

[13] S. Yüksel, N. Kabay, M. Yüksel, Removal of Bisphenol A (BPA) from water by various nanofiltration (NF) and reverse osmosis (RO) membranes, J. Hazard. Mater., 263 (2013) 307–310.

[14] F. Khazaali, A. Kargari, M. Rokhsaran, Application of low-pressure reverse osmosis for effective recovery of Bisphenol A from aqueous wastes, Desal. Water Treat., 52 (2013) 7543–7551.

[15] B. Van der Bruggen, Chemical modification of polyether sulfone nanofiltration membranes: a review, J. Appl. Polym. Sci., 114 (2009) 630–642.

[16] W.F. Zhao, J.Y. Huang, B.H. Fang, S.Q. Nie, N. Yi, B.H. Su, H.F. Li, C.S. Zhao, Modification of polyethersulfone membrane by blending semi-interpenetrating network polymeric nanoparticles, J. Membr. Sci., 369 (2011) 258–266.

[17] H. Susanto, M. Ulbricht, Characteristics, performance and stability of polyethersulfone ultrafiltration membranes prepared by phase separation method using different macromolecular additives, J. Membr. Sci., 327 (2009) 125–135.

[18] D.B. Zhi, W. Lin, G.N. Yun, The removal of Bisphenol A by ultrafiltration, Desalination. 221 (2008) 312–317.

[19] D. Bing-Zhi, W. Lin, G. Nai-Yun, The removal of Bisphenol A by hollow fiber microfiltration membrane, Desalination, 250 (2010) 693–697.

[20] G. Gnanasekaran, S. Balaguru, G. Arthanareeswaran, B.D. Diganta, Removal of hazardous material from wastewater by using metal organic framework (MOF) embedded polymeric membranes, Sep. Sci. Technol., 54 (2018) 434–446.

[21] J.Y. Heo, J.R.V. Flora, N. Her, Y.-G. Park, J.W. Cho, A. Son, Y.M. Yoon, Removal of Bisphenol A and 17β-estradiol in single walled carbon nanotubes–ultrafiltration (SWNTs–UF) membrane systems, Sep. Purif. Technol., 90 (2012) 39–52.

[22] L.D. Nghiem, D. Vogel, S. Khan, Characterising humic acid fouling of nanofiltration membranes using Bisphenol A as a molecular indicator, Water Res., 42 (2008) 4049–4058.

[23] S.A. Kiran, Y.L. Thuyavan, G. Arthanareeswaran, T. Matsuura, A.F. Ismail, Impact of graphene oxide embedded polyethersulfone membranes for the effective treatment of distillery effluent, Chem. Eng. J., 286 (2016) 528–537.